Journal of Integrative Neuroscience

J. Integr. Neurosci. **2026**; 25(7): 51032
https://doi.org/10.31083/JIN51032

Original Research

Dl-3-n-Butylphthalide Protects Human Brain Microvascular Endothelial Cells Against Ischemic Injury Through Dual Modulation of HIF1α/VEGF-Mediated Angiogenesis and COX2-Mediated Inflammation

Yanyan Wang[1,2,3,†], Chuanxin Su[4,†], Teng Chen[1], Shijia Chen[5], Zhenzhong Li[1,2,3], Lihong Zhang[1,2,3,*]

[1]Department of Neurology, The Second Hospital of Hebei Medical University, 050000 Shijiazhuang, Hebei, China
[2]The Key Laboratory of Neurology (Hebei Medical University), Ministry of Education, 050000 Shijiazhuang, Hebei, China
[3]Neurological Laboratory of Hebei Province, 050000 Shijiazhuang, Hebei, China
[4]Department of Rheumatology and Immunology, Peking University People's Hospital Qingdao Hospital, 266011 Qingdao, Shandong, China
[5]Institute of System Medicine, Zhejiang University School of Medicine, 310000 Hangzhou, Zhejiang, China
*Correspondence: lihongzhang@hebmu.edu.cn (Lihong Zhang)
[†]These authors contributed equally.
Academic Editor: Bettina Platt
Submitted: 14 February 2026 Revised: 3 April 2026 Accepted: 9 May 2026 Published: 21 July 2026

Abstract

Background: Stroke remains a leading cause of death and disability worldwide. Endothelial dysfunction plays a central role in both acute ischemic injury and subsequent recovery. In this study, we investigated the protective effects and underlying mechanisms of Dl-3-n-butylphthalide (NBP) on human brain microvascular endothelial cells (HBMECs) subjected to oxygen-glucose deprivation (OGD), an *in vitro* model of ischemic stroke. **Methods:** HBMECs were divided into three groups: control (normoxia), OGD (10 h hypoxia, followed by reoxygenation for different durations (0–24 h), and then a subsequent 24 h incubation), and NBP-treated OGD (10 μmol/L NBP during reoxygenation). Cell viability and apoptosis were assessed by Cell Counting Kit 8 (CCK8), lactate dehydrogenase (LDH) release, and flow cytometry. Mitochondrial function was evaluated using MitoTracker fluorescence. Molecular mechanisms were examined using Western blot, quantitative real-time PCR (qRT-PCR), immunofluorescence, and enzyme-linked immunosorbent assay (ELISA), focusing on the hypoxia-inducible factor-1α (HIF1α)/vascular endothelial growth factor (VEGF) angiogenic pathway and cyclooxygenase-2 (COX2)-mediated inflammatory response. **Results:** NBP at 10 μmol/L significantly improved HBMEC viability (37.5% increase, $p < 0.01$), reduced apoptosis ($p < 0.01$), and restored mitochondrial membrane potential ($p < 0.05$) following OGD injury. Mechanistically, NBP demonstrated dual pathway modulation by: (1) promoting angiogenesis-related gene expression through HIF1α upregulation and subsequent increase in vascular endothelial growth factor receptor 2 (VEGFR2) and endothelial nitric oxide synthase (eNOS) expression ($p < 0.05$); and (2) suppressing inflammation via COX2 downregulation with concurrent reduction of downstream mediators including inducible nitric oxide synthase (iNOS), tumor necrosis factor-α (TNFα), interleukin-1β (IL-1β), and Thromboxane B_2 (TXB_2, $p < 0.05$). This coordinated regulation created a favorable microenvironment balancing pro-angiogenic signals with anti-inflammatory effects. **Conclusion:** NBP exerts multi-targeted protection on HBMECs after ischemic injury through associated with the activation of HIF1α/VEGF-mediated angiogenesis and suppression of COX2-driven inflammation. This dual modulation strategy, targeting both vascular repair and inflammatory control, provides preliminary *in vitro* mechanistic insights that warrant further validation *in vivo* and in clinical settings.

Keywords: ischemic stroke; human brain microvascular endothelial cells; Dl-3-n-butylphthalide; angiogenesis; inflammation

1. Introduction

Stroke is recognized as the second leading cause of death worldwide and a major contributor to disability, creating a significant economic burden on individuals, families, and healthcare systems [1]. Given the high incidence and severe consequences of stroke, there is an urgent need for cost-effective post-stroke interventions to improve recovery outcomes. Currently, treatment strategies for acute stroke are primarily limited to reperfusion therapies, such as tissue plasminogen activator (tPA) and mechanical thrombectomy, which do not address the underlying mechanisms of stroke-related brain injury [2,3].

Recent advances in stroke research have highlighted the importance of the neurovascular unit (NVU), which consists of neurons, endothelial cells, astrocytes, and pericytes, in understanding stroke pathology [4,5]. This concept emphasizes that ischemic injury does not solely affect neurons but also disrupts vascular integrity and glial cell function. Endothelial cells (ECs) are crucial components of the NVU, playing a pivotal role in maintaining cerebral

blood flow and metabolic homeostasis. Atherosclerosis, a primary risk factor for stroke, is associated with increased EC apoptosis, highlighting the need for therapies that preserve endothelial health [6].

Among them, promoting angiogenesis (i.e., the formation of new blood vessels) and eliminating inflammatory responses have been proven to be associated with improved functional recovery and reduced recurrence rate after a stroke. The hypoxia-inducible factor-1α (HIF1α)/vascular endothelial growth factor (VEGF) pathway and the cyclooxygenase-2 (COX2)/inducible nitric oxide synthase (iNOS) pathway are key regulators of angiogenesis and inflammation, respectively. Notably, these two pathways often interact under ischemic conditions, where excessive inflammation can impair HIF1α signaling and VEGF-mediated vascular repair [7,8]. Therefore, simultaneously targeting both pathways may represent a more effective therapeutic strategy. By stimulating the activity of HIF1α, it can increase the expression of vascular growth factors, stimulate the formation of new blood vessels, enhance cerebral blood flow and prevent ischemic damage. COX2, as a central factor influencing inflammation, its inhibition will affect the expression of iNOS, thereby eliminating inflammation [9,10].

Traditional treatment approaches for stroke, which often follow a "one-size-fits-all" model, may not fully address the complex nature of stroke and its effects on the NVU. In contrast, traditional Chinese medicine, known for its multi-targeted strategies, presents promising alternatives for managing stroke. One such agent is Dl-3-n-butylphthalide (NBP), a synthetic compound derived from natural sources that has emerged as a novel therapeutic option for cerebrovascular diseases by targeting various pathways and mechanisms [11]. Research has shown that NBP can enhance cerebral microvascular function, improve regional blood flow, and promote angiogenesis, indicating its potential role in stroke prevention and recovery [12,13].

However, despite these encouraging findings, the specific effects of NBP on endothelial cells, especially in the context of ischemic injury, have not been thoroughly investigated. Therefore, this study aims to explore the direct effects of NBP on human brain microvascular endothelial cells (HBMECs) subjected to oxygen-glucose deprivation (OGD), a widely used *in vitro* model for ischemic stroke. We will evaluate how NBP influences HBMEC viability, apoptosis rates, and mitochondrial function, along with the signaling pathways involved in these protective effects. By clarifying the mechanisms through which NBP operates, this research aspires to enhance the development of more effective therapeutic strategies for managing ischemic stroke.

In conclusion, the ongoing investigation into the NVU, endothelial cell health, and the diverse approaches offered by traditional Chinese medicine, such as NBP, holds significant potential for improving stroke treatment. This study aims to investigate the protective effects of NBP on HBMECs following ischemic injury and to elucidate the underlying molecular mechanisms involving HIF1α/VEGF-mediated angiogenesis and COX2-mediated inflammation.

2. Experimental Methods

2.1 Cell Culture

HBMECs (Cat. HTX1843, Otwo Biotech, Shenzhen, Guangdong, China; RRID: CVCL_U985) were maintained in high-glucose DMEM supplemented with 10% fetal bovine serum (FBS, Cat. 10099141C, Gibco, Grand Island, NY, USA) and 1% penicillin-streptomycin (Cat. 15140122, Gibco) at 37 °C in a 5% CO_2 humidified incubator. The medium was refreshed every 48 hours. Upon reaching >80% confluency, cultures were rinsed with 0.01 M phosphate-buffered saline (PBS) and detached using 0.25% trypsin-EDTA (Cat. C0201, Beyotime, Shanghai, China). Prior to experimental use, all cells tested negative for mycoplasma contamination (Mycoplasma Detection Kit, Cat. Myco-P-20, Biothrive Sci. & Tech., Shanghai, China), authenticated by STR profiling, and were restricted to passages 2–8.

2.2 Oxygen-Glucose Deprivation (OGD) Model

The OGD model was used to simulate cerebral ischemia-reperfusion injury. Briefly, cells were cultured in a DMEM glucose-free medium (Gibco) planted in a plate. Cells were sealed in anaerobic culture bags (Cat. R686010, distributed by Thermo Fisher Scientific, Eugene, OR, USA; manufactured by Mitsubishi Gas Chemical, Tokyo, Japan) containing an anaerobic gas-generating pouch (95% N_2, 5% CO_2) and an oxygen indicator and incubated at 37 °C for 10 h. The indicator remained colorless, confirming successful anaerobic conditions. Following this, the bags with plates were transferred to a 5% CO_2 incubator for varying durations (0, 6, 8, 10, 12, or 24 h). After combined glucose deprivation and hypoxia treatment, the anaerobic devices were removed, and cells were switched to complete medium and cultured under standard conditions (37 °C, 5% CO_2) for an additional 24 h.

2.3 NBP Treatment and Cell Viability Assay

NBP active pharmaceutical ingredients (API) were provided by Shijiazhuang Pharmaceutical Group NBP Pharmaceutical Co., Ltd (Cat. 518190403, Shijiazhuang, Hebei, China). Firstly, it was completely dissolved with dimethyl sulfoxide (DMSO) (Cat. ST038; Beyotime) to a concentration of 1 mM solution for use. The standby solution was diluted with DMEM at different concentrations of 1000 μM, 100 μM, 10 μM, 1 μM, and 0.1 μM. Interventions with different concentrations of NBP were performed for 24 h followed by HBMEC OGD treatment. Besides, the final concentration of DMSO was less than 0.2%. Cell viability was evaluated using Cell Counting Kit 8 (CCK8) (Dojindo, Kumamoto, Japan) according to the manufacturer's recom-

mendations. Cells were cultured in a medium containing 10% CCK8 for 2.5 h. Finally, absorbance was measured at a wavelength of 450 nm using a microplate reader to select the most appropriate concentration for subsequent experiments based on cell viability.

Lactate dehydrogenase (LDH) activity was assessed in both intracellular and extracellular (cell culture medium) samples using a commercial LDH assay kit (Cat.D799207, Sangon Biotech, Shanghai, China) following the manufacturer's protocol. Results were calculated by reference to standard curves.

2.4 Detection of Apoptosis by Flow Cytometry

Apoptosis was assessed using the PE Annexin V Apoptosis Detection Kit I (Cat. 559763, BD Pharmingen, San Diego, CA, USA). Cells were harvested, resuspended in 100 µL of 1× annexin-binding buffer, and incubated with 5 µL of PE Annexin V and 5 µL of 7-AAD for 15 min at room temperature in the dark. The reaction was terminated by adding 400 µL of 1× annexin-binding buffer. Flow cytometric analysis was performed on a CytoFLEX LX (Beckman Coulter, Brea, CA, USA), and data were processed using CytExpert software (v 2.3, Beckman Coulter, Brea, CA, USA). A minimum of 10,000 cells per sample was analyzed.

2.5 Mitochondrial Probe Assay

Glass coverslips were used to hold the cells in 6-well cell culture plates. And after OGD and NBP treatments, different groups of the cell coverslips were stained with Mito-Tracker (Cat. M22425, Thermo Fisher Scientific) (stock solution 1mM) 1:5000 dilution at 37 °C for 30 min. Cells were washed with PBS and fixed with 3.2% cold paraformaldehyde (PFA), (Cat. 80096618, Sinopharm Chemical Reagent Co., Ltd., Shanghai, China) at room temperature for 20 min. After washing, the glass coverslips were placed upside down on the slides. The slides were sealed and stored away from light in a 4 °C refrigerator. Finally, we observed the slides under a laser-scanning confocal microscope (Olympus FV1200, Olympus Corporation, Tokyo, Japan). Five non-overlapping fields per coverslip were randomly selected under 200× magnification. Fluorescence intensity was measured using ImageJ software (v1.53, National Institutes of Health, Bethesda, MD, USA) by quantifying the mean pixel intensity per field after background subtraction. Results are expressed as relative fluorescence units (RFU) normalized to the control group. The number of samples is n = 3.

2.6 Western Blot Analysis

The total proteins of the cells in each group were extracted by adding 0.5 mL of frozen radioimmunoprecipitation assay (RIPA) (Cat. No. P0013B; Beyotime) buffer with a cocktail of protease (Cat. 04693159001) and phosphatase inhibitors (Cat. 04906837001, Roche, Basel, Switzerland) to the culture dish. After centrifugation at 12,000 rpm for 30 min at 4 °C, protein concentrations were determined using the bicinchoninic acid (BCA) Protein Assay Kit (Cat. P0009; Beyotime). Equal amounts of protein (20 µg per lane) were separated by sodium dodecyl sulfate–polyacrylamide gel electrophoresis (SDS-PAGE). We prepared 2 g/L proteins in PBS in each tube, and then added 5× SDS loading buffer (Cat. P0015; Beyotime) to each sample. Then, each tube was boiled at 100 °C for 5 min. Electrophoresis (200 V) was performed with 10%–15% SDS-PAGE gels (Cat. FD2001, Fude Biotech, Hangzhou, Zhejiang, China). Electrophoresis was terminated when the loading dye reached the bottom of the gel, and then the loading dye was transferred to polyvinylidene fluoride (PVDF) membranes (Cat. IPVH00010, Millipore, Billerica, MA, USA) on a Bio-Rad transfer device at 300 mA for 60 min. After sealing the cell membranes with 5% skim milk powder at room temperature for 3 h, the PVDF membranes were incubated with primary antibodies at 4 °C overnight. The primary antibodies included COX2 antibody (1:1000, Cat. ab15191, Abcam, Cambridge, UK), HIF1α antibody (1:1000, Cat. 36169, CST, Danvers, MA, USA), vascular endothelial growth factor receptor 2 (VEGFR2) antibody (1:1000, Cat. 9698,CST), iNOS antibody (1:500, Cat. AF6007; Affinity Biosciences, Cincinnati, OH, USA), interleukin-1β (IL-1β, 1:1000, Cat. 31202, CST), tumor necrosis factor-α (TNFα, 1:1000, Cat.11948, CST, Danvers, MA, USA) and GAPDH antibody (1:1000, Cat. 2118, CST). After incubation time, PVDF membranes were rinsed with tris-buffered saline with Tween 20 (TBST) for 4 × 5 min and incubated with horseradish peroxidase-coupled secondary antibodies for 2.5 h at room temperature. Secondary antibodies were goat anti-rabbit antibody (1:5000, Cat.BK-R050, Bioker, Oviedo, Asturias, Spain) and goat anti-mouse antibody (1:5000, Cat.BK-M050, Bioker). Protein bands were visualized using the ChemiDoc Touch Imaging System (Bio-Rad, Hercules, CA, USA) after enhanced chemiluminescence (ECL) incubation. Band intensities were quantified with Image Lab software (v6.1, Bio-Rad). All experiments were conducted in triplicate.

2.7 Enzyme Linked Immunosorbent Assay

Following OGD/reperfusion (OGD/R) treatment with or without NBP exposure, cells were collected and culture supernatants were harvested. Thromboxane B_2 (TXB_2, Cat# D711360) and nitric oxide (NO, Cat# D799310) levels were measured using commercial assay kits (Sangon Biotech) according to manufacturer protocols. Data were quantified based on standard curves.

2.8 Quantitative RT-PCR

Quantitative real-time PCR (qRT-PCR) was performed on a Rotor-Gene Q real-time PCR cycler (QIAGEN, Hilden, Germany) using 1 µg of total RNA with the QuantiTect SYBR Green RT-PCR Kit (Cat. 204243, QIA-

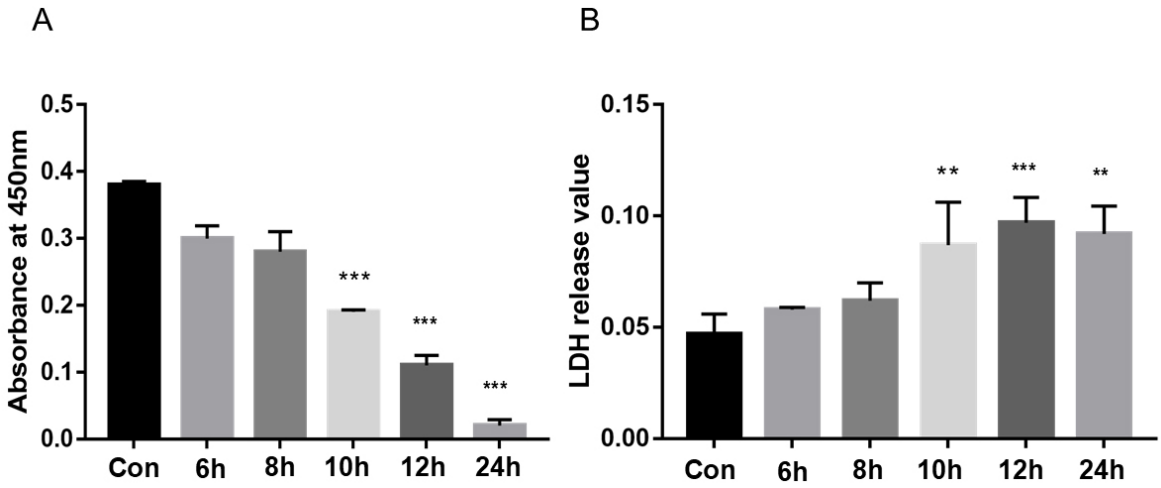

Fig. 1. Assessment of HBMEC viability. CCK8 assay (A) and cytotoxicity using LDH release assay (B) after exposure to OGD for indicated time periods (0, 6, 8, 10, 12, and 24 h). Data are expressed as mean ± SEM of three independent experiments. $^{**}p < 0.01$ versus 0 h control. $^{***}p < 0.001$ versus 0 h control. Con, control; HBMEC, human brain microvascular endothelial cell; CCK8, Cell Counting Kit 8; LDH, lactate dehydrogenase; OGD, oxygen-glucose deprivation; SEM, standard error of the mean.

GEN, Hilden, Germany) following the manufacturer's instructions. All reactions were performed in technical duplicate, and data were acquired and analyzed using Rotor-Gene Q Series Software (v2.3.5, QIAGEN, Hilden, Germany).

All experiments included at least three independent biological replicates. The primer-pairs used for RT-qPCR were *GAPDH*: (primers ACAGTCAGCCGCATCTTCTT and TTGATTTTGGAGGGATCTCG), Vascular Endothelial Growth Factor A (*VEGFA)* (AGGGCAGAATCATCACGAAGT and AGGGTCTCGATTGGATGGCA), nuclear factor kappa B (*NFκB*) (AACAGAGAGGATTTCGTTTCCG and TTTGACCTGAGGGTAAGACTTCT), TNFα (CCTCTCTCTAATCAGCCCTCTG and GAGGACCTGGGAGTAGATGAG), endothelial nitric oxide synthase (*eNOS*) (TGATGGCGAAGCGAGTGAAG and ACTCATCCATACACAGGACCC), iNOS (TTCAGTATCACAACCTCAGCAAG and TGGACCTGCAAGTTAAAATCCC), *IL-1β* (ATGATGGCTTATTACAGTGGCAA and GTCGGAGATTCGTAGCTGGA). Gene expression was normalized to *GAPDH* as an internal control, and relative expression levels were calculated using the $2^{-\Delta\Delta Ct}$ method.

2.9 Immunofluorescence Staining

Cells grown on coverslips were fixed with freshly prepared 4% paraformaldehyde in PBS (pH 7.4) for 40 min, then washed in PBS for 5 min and permeabilized with 2% Triton X-100 (Sinopharm Chemical Reagent Co., Ltd., Shanghai, China) for 15 min. The cells were incubated with primary antibodies (rabbit anti-HIF1α 1:250 dilution, Cat. 36169, CST) overnight at 4 °C after the non-specific binding sites were blocked with 5% bovine serum albumin (BSA, Cat. SW3015, Solaria, Shanghai, China) blocking solution for 30 min. After washing in PBS for 3 × 5 min, the cells were incubated with secondary antibodies (Alexa Fluor488, Cat. A-11008; Thermo Fisher Scientific) for 1.5 h at room temperature and then washed with PBS for 3 × 5 min at room temperature. The slides were incubated with 15 µL of DAPI (Cat. H-1200-10, Vector Laboratories, Burlingame, CA, USA), and the coverslips full of cells incubated with the antibody were placed on the slides. The sections of controls (following the same procedure except for the addition of primary antibodies) showed no signal. The slides were examined under a fluorescent microscope (Olympus VS120, Olympus Corporation, Tokyo, Japan). Five sections were randomly selected from each slide, and their intensity was analyzed using ImageJ software (v1.53, National Institutes of Health).

2.10 Statistical Methods

All data are presented as mean ± standard error of the mean (SEM). Statistical analyses were performed using one-way ANOVA followed by Tukey's post hoc test for multiple comparisons between groups (SPSS 22.0, IBM Corp., Armonk, NY, USA). Statistical significance was defined as $p < 0.05$.

3. Results

3.1 NBP Reduced the Apoptotic Rate in HBMECs After OGD Injury

To investigate the protective effects of NBP on HBMECs following OGD, we established an OGD/R model using HBMECs. Cell viability and apoptosis were subsequently evaluated. CCK8 assay showed the metabolic activity of the cells had significantly decreased ($p < 0.001$) (Fig. 1A), and LDH assay revealed that after OGD 10 h,

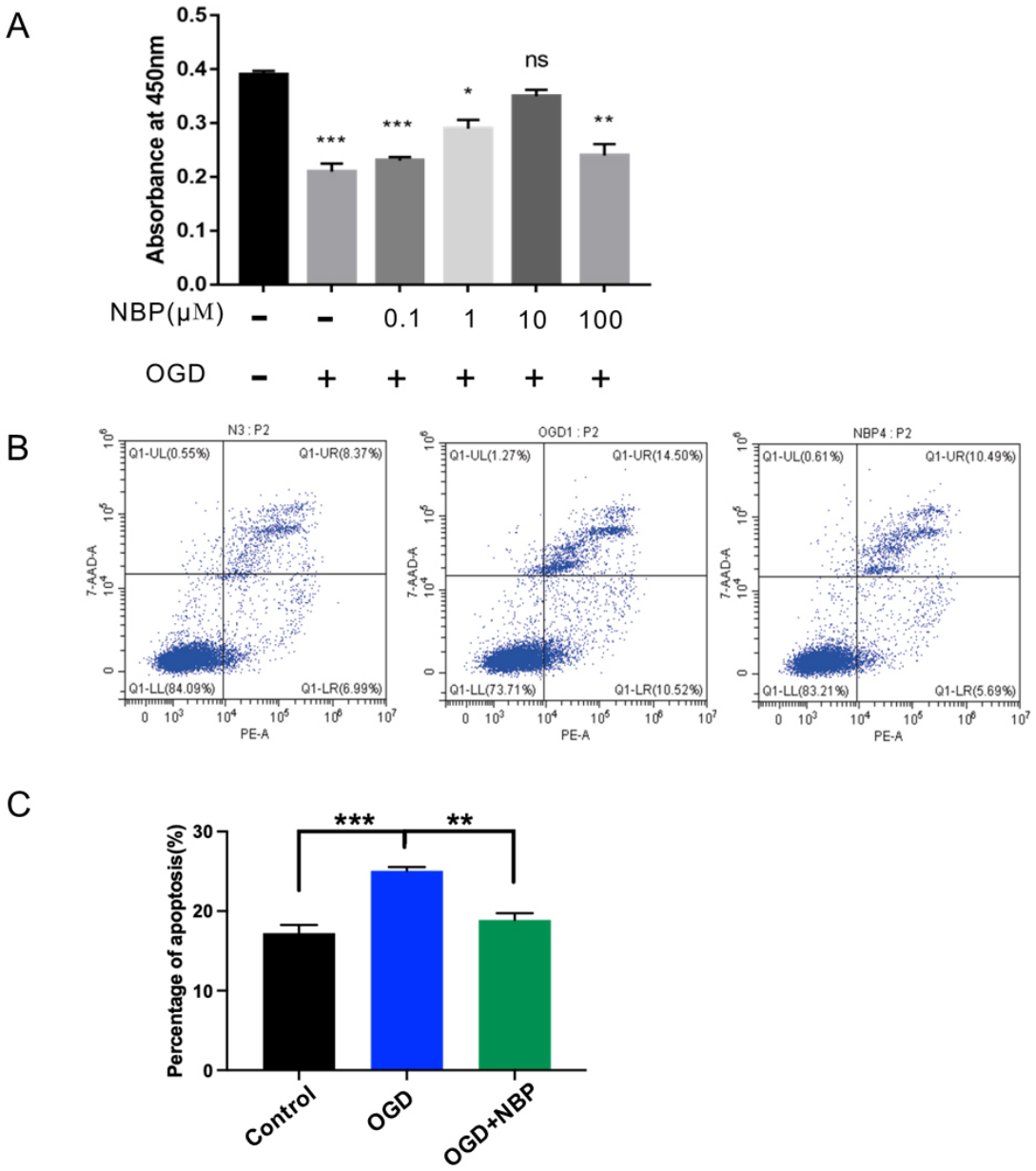

Fig. 2. Effects of different concentrations of NBP on cell viability and apoptosis after OGD. (A) HBMEC viability assessed by CCK8 assay after treatment with five different NBP concentrations (0, 0.1, 1, 10, 100 μM) following 10 h OGD exposure. (B) Flow cytometry analysis of apoptosis after staining with PE-Annexin V/7-AAD (FSC/SSC, FSC-A/FSC-H, PE-Annexin V/7-AAD). Representative scatter plots show Annexin V (x-axis) vs 7-AAD (y-axis). Q1-UL: necrotic cells; Q1-UR: late apoptotic cells; Q1-LL: viable cells; Q1-LR: early apoptotic cells. (C) Percentage of total apoptotic cells of different groups. Data were expressed as mean ± SEM (n = 3). $^{*}p < 0.05$, $^{**}p < 0.01$, $^{***}p < 0.001$ vs Control. ns: not significant. NBP, Dl-3-n-butylphthalide; PE-Annexin V/7-AAD, phycoerythrin-conjugated Annexin V and 7-Aminoactinomycin D.

compared with control cells, LDH release increased significantly ($p < 0.01$) (Fig. 1B), indicating enhanced cytotoxicity. Thus, we used 10 h as the intervention time of the subsequent OGD model.

To further determine the protective effect of NBP on OGD injury, the concentration of NBP should first be tested. Under OGD/R conditions, NBP treatment enhanced cell viability by 37.5% at the concentration of 10 μmol/L (Fig. 2A). Then, we used flow cytometric analysis to test the apoptosis in HBMECs. As shown in Fig. 2B, the total apoptotic rate in HBMECs after OGD was significantly increased ($p < 0.001$) compared to controls, while the total apoptotic rate was found to be significantly decreased ($p < 0.01$) after OGD in the NBP intervention group (Fig. 2B,C). So we chose 10 μmol/L NBP for further experiments.

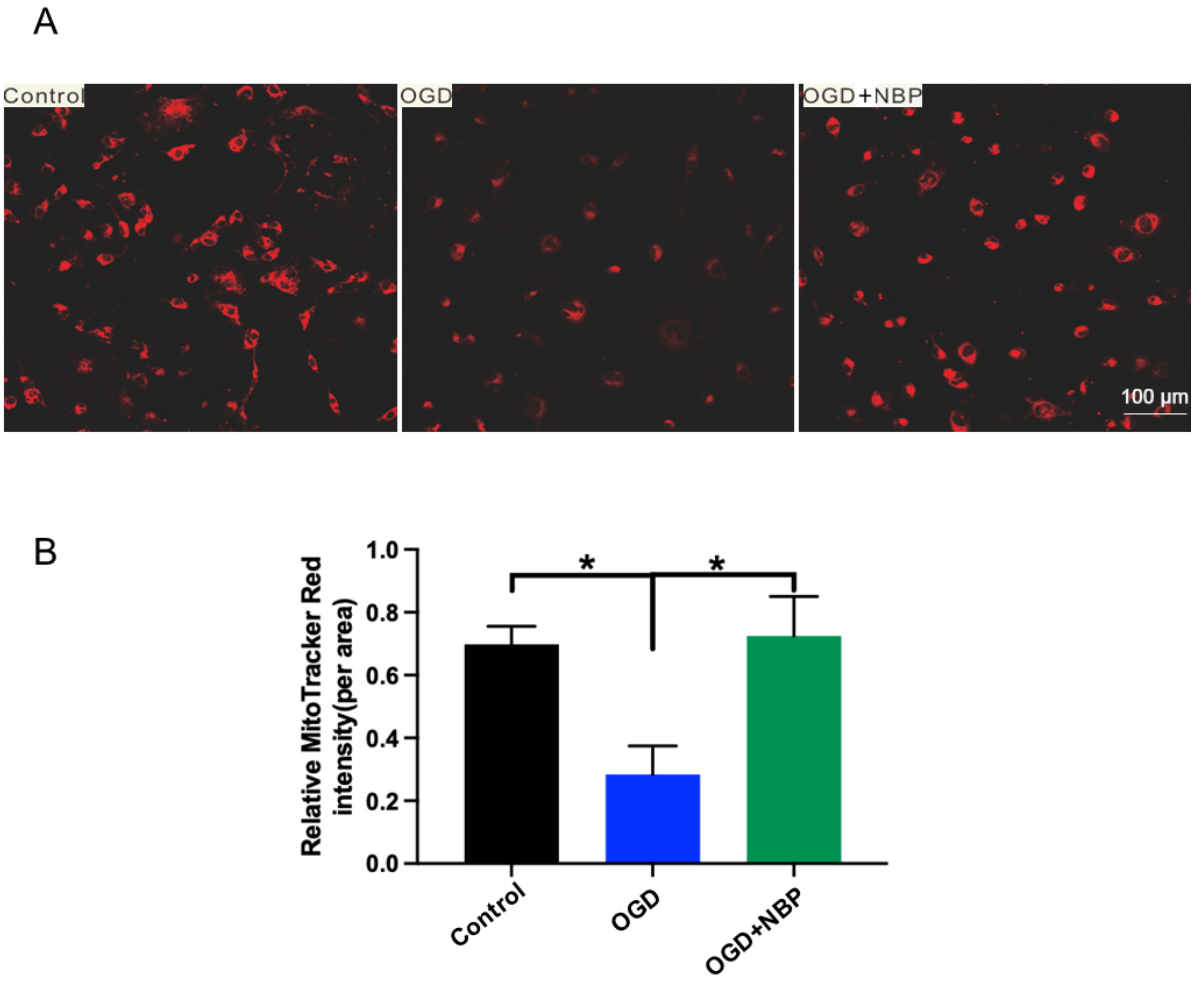

Fig. 3. NBP protects against OGD-induced mitochondrial damage. (A) Representative fluorescence images of HBMECs stained with MitoTracker Red (red fluorescence), magnification ×200. (B) Quantitative analysis of relative MitoTracker Red fluorescence intensity per area. Data are expressed as mean ± SEM (n = 3). $^{*}p < 0.05$. Scale bar: 100 μm.

3.2 Mitochondrial Protective Effect of NBP on HBMECs After OGD Injury

To further explore the mechanism by which NBP reverses OGD-induced HBMECs apoptosis, we tested the fluorescence intensity of mitochondria. Mitochondrial membrane integrity was assessed using MitoTracker staining in live cells. As shown in Fig. 3A,B, mitochondrial fluorescence intensity was significantly decreased by approximately 60% in the OGD group compared to the control group ($p < 0.05$), indicating substantial mitochondrial damage following OGD injury. NBP intervention significantly reversed this decrease ($p < 0.05$), restoring mitochondrial fluorescence intensity to approximately 104% of Control levels. These results suggest that NBP effectively attenuates OGD-induced mitochondrial damage in HBMECs.

3.3 NBP Upregulates HIF1α/VEGF Pathway-Related Gene and Protein Expression Under OGD Conditions

Immunofluorescence and Western blot analyses demonstrated that HIF1α expression in HBMECs was low under normal conditions. In the OGD model, HIF1α expression showed a modest increase compared to the control group, but this change did not reach statistical significance ($p > 0.05$). Following NBP intervention, HIF1α expression was significantly upregulated compared to the OGD group, with approximately 2.01-fold increase in immunofluorescence intensity ($p < 0.01$, Fig. 4A) and approximately 1.39-fold increase in protein expression by Western blot ($p < 0.01$, Fig. 4B). Consistent with HIF1α upregulation, downstream components of the VEGF signaling pathway were also significantly activated by NBP treatment: VEGFR2 protein expression increased approximately 1.24-fold ($p < 0.05$, Fig. 4B, the original Western blot images are available in the **Supplementary Material**), while *VEGFA* and *eNOS* mRNA levels increased approximately 1.18-fold and 1.28-fold, respectively ($p < 0.05$, Fig. 4C). These results indicate that NBP upregulates HIF1α expression, thereby activating the downstream VEGF signaling pathway in OGD-injured HBMECs.

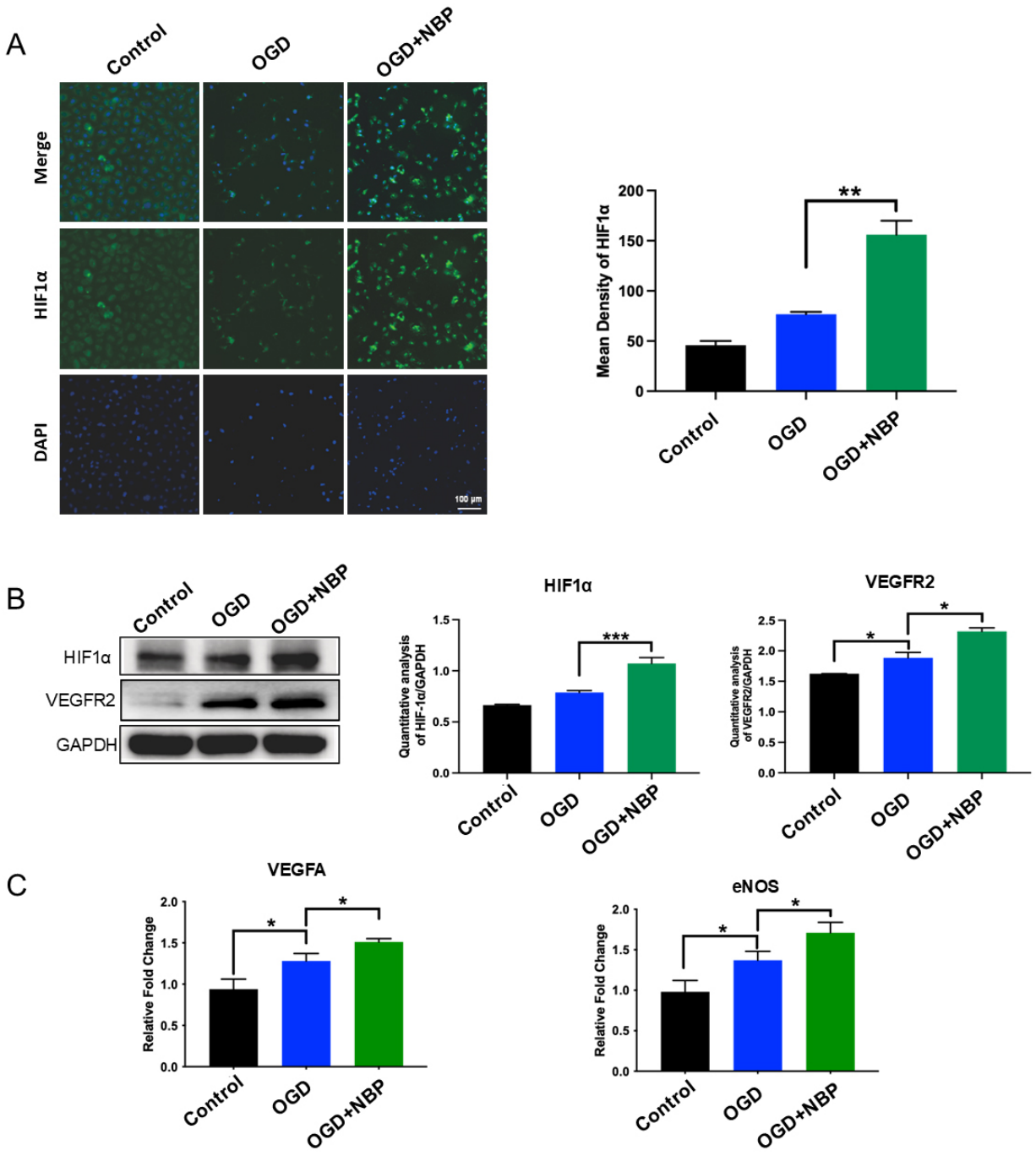

Fig. 4. NBP promotes angiogenesis-related protein expression under OGD conditions. (A) Representative immunofluorescence images of HIF1α (green) and DAPI (blue) staining. Merged images are shown in the top panel. Quantification of mean fluorescence density of HIF1α positive cells is shown in the right panel. Scale bar: 100 μm. (B) Representative Western blot images and densitometric quantification of HIF1α and VEGFR2 protein expression normalized to GAPDH. (C) qRT-PCR analysis of *VEGFA* and *eNOS* mRNA expression levels. Data were expressed as mean ± SEM (n = 3). $^{*}p < 0.05$, $^{**}p < 0.01$, $^{***}p < 0.001$. HIF1α, hypoxia-inducible factor-1α; VEGFR2, vascular endothelial growth factor receptor 2; qRT-PCR, quantitative real-time PCR; VEGFA, Vascular Endothelial Growth Factor A; eNOS, endothelial nitric oxide synthase.

3.4 NBP Inhibited the Expression of OGD-Induced Inflammatory Markers by COX2-iNOS Signaling

NBP also exhibited significant anti-inflammatory effects in OGD-injured HBMECs. Western blot analysis revealed that COX2 protein expression was markedly elevated following OGD, and NBP treatment reduced COX2 expression by approximately 46% compared to the OGD group ($p < 0.01$, Fig. 5A, the original Western blot im-

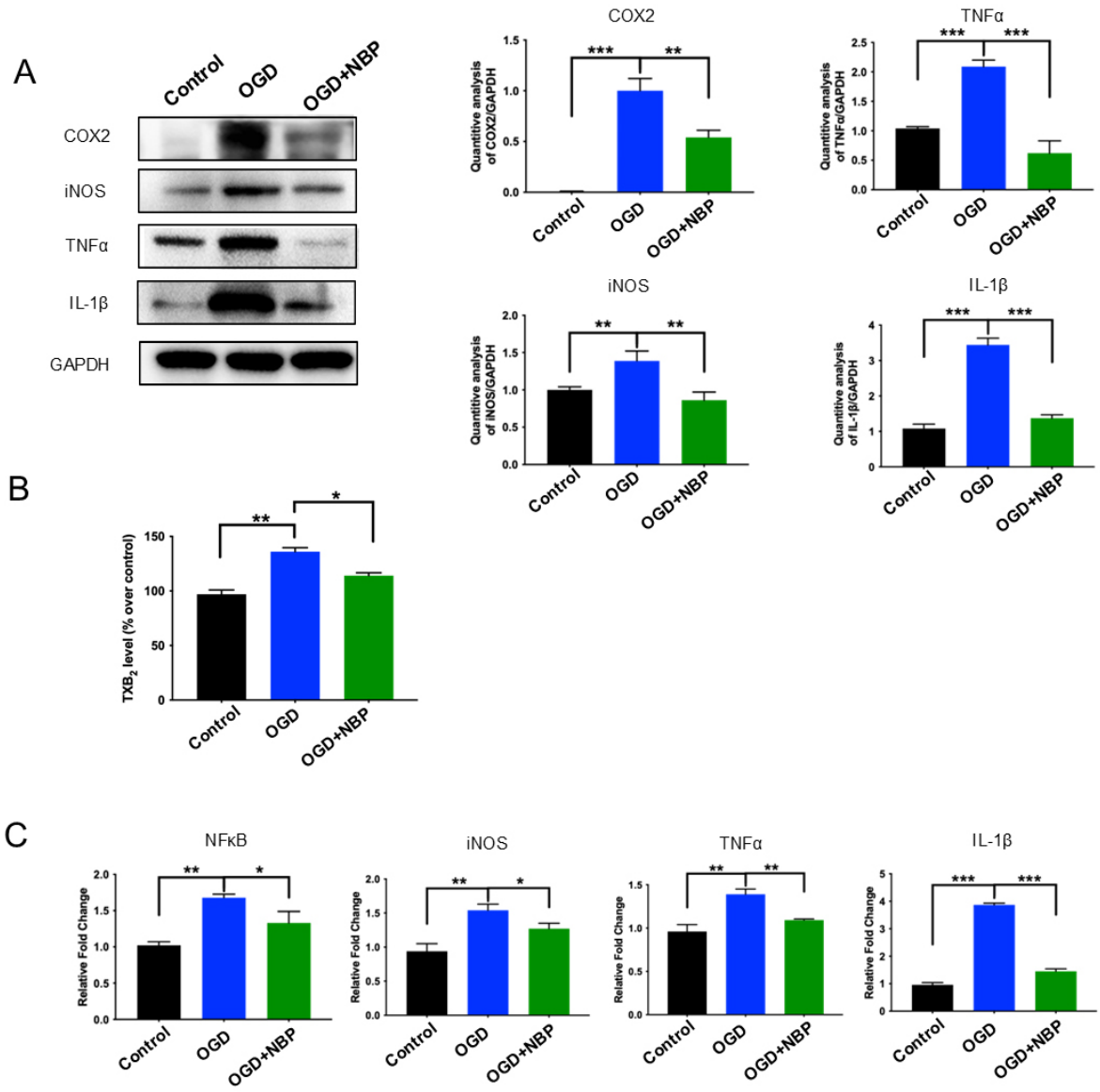

Fig. 5. NBP attenuates OGD induced inflammatory response. (A) Representative Western blot images and densitometric quantification of COX2, iNOS, TNFα, and IL-1β protein expression levels normalized to GAPDH. (B) Enzyme-linked immunosorbent assay (ELISA) results showing TXB_2 production levels. (C) qRT-PCR analysis of *NFκB*, *iNOS*, *TNFα*, and *IL-1β* mRNA expression levels. Data are expressed as mean ± SEM (n = 3). $^{*}p < 0.05$, $^{**}p < 0.01$, $^{***}p < 0.001$. COX2, cyclooxygenase-2; iNOS, inducible nitric oxide synthase; TXB_2, Thromboxane B_2; TNFα, tumor necrosis factor-α; IL-1β, interleukin-1β; NFκB, nuclear factor kappa B.

ages are available in the **Supplementary Material**). Similarly, the protein expression of other inflammatory mediators was also significantly suppressed by NBP: TNFα decreased by approximately 72%, IL-1β by approximately 58%, and iNOS by approximately 38.6% compared to the OGD group (all $p < 0.01$, Fig. 5A).

Since TXB_2 is a stable metabolite of TXA_2 and a downstream product of the COX2 pathway, we measured TXB_2 levels by ELISA as a functional indicator of COX2 activity. NBP treatment reduced TXB_2 concentration by approximately 16% compared to the OGD group ($p < 0.05$, Fig. 5B). Furthermore, qRT-PCR analysis showed that the mRNA expression of inflammatory mediators was significantly decreased following NBP treatment, including *NFκB*, *TNFα*, *IL-1β*, (decreased by approximately 20%) and iNOS (decreased by approximately 70%) (all $p < 0.05$, Fig. 5C). Collectively, these results demonstrate that NBP attenuates the OGD-induced inflammatory response in HBMECs at both the protein and transcriptional levels.

4. Discussion

Stroke remains a leading cause of death and disability worldwide, with endothelial dysfunction playing a central role in both acute injury and recovery phases. This study

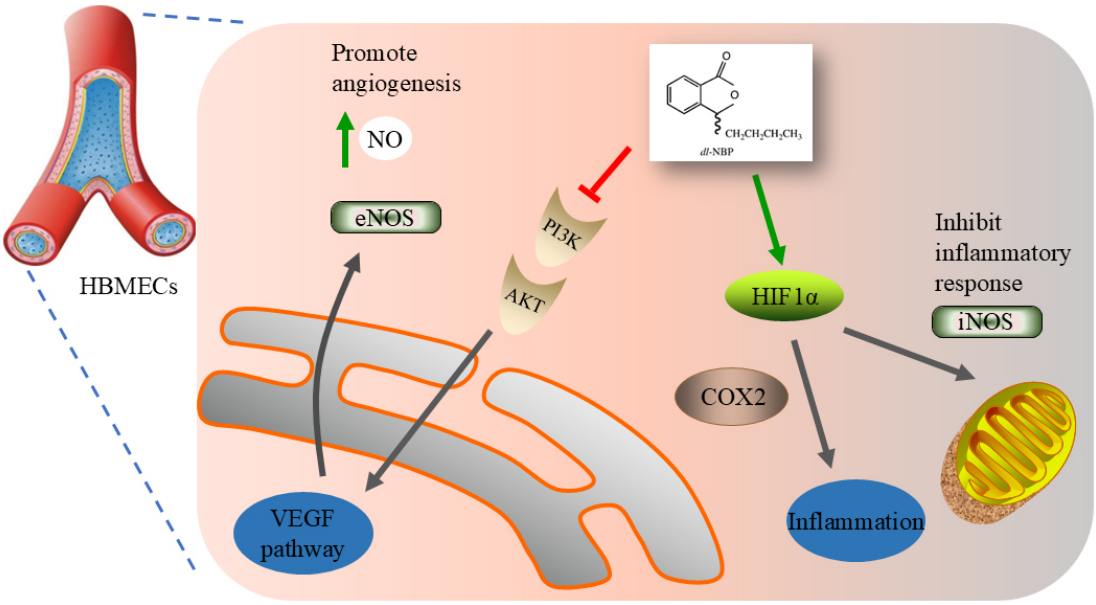

Fig. 6. Schematic illustration of the protective mechanisms of NBP in HBMECs under OGD conditions. NBP activates HIF1α signaling, which promotes angiogenesis through upregulation of eNOS/NO and the VEGF pathway, while simultaneously inhibiting inflammatory responses by suppressing COX2, iNOS, and pro-inflammatory cytokines. These combined effects protect mitochondrial function and enhance endothelial cell survival. Putative signaling pathways involved in NBP-mediated protection. Dashed lines indicate proposed mechanisms based on prior literature, which require further experimental validation in this model. PI3K, phosphatidylinositol 3-kinase; AKT, protein kinase B.

demonstrates that NBP protects HBMECs against OGD through multiple complementary mechanisms: enhancing cell viability, reducing apoptosis, preserving mitochondrial function, promoting angiogenesis via the HIF1α/VEGF pathway, and suppressing inflammation through COX2 modulation. These findings provide correlative mechanistic insights into NBP's protective effects on endothelial cells under ischemic conditions *in vitro*.

In our study, NBP treatment reversed the OGD-induced decline in MitoTracker Red fluorescence intensity (Fig. 3), indicating preservation of mitochondrial membrane potential. Loss of mitochondrial membrane potential is a well-established early event in the intrinsic apoptotic cascade, typically followed by cytochrome c release, caspase activation, and increased reactive oxygen species (ROS) production [14,15]. Although we did not directly measure cytochrome c release or ROS levels in the present study, the observed preservation of mitochondrial membrane potential by NBP suggests that these downstream apoptotic events may also be attenuated, a hypothesis that warrants direct verification in future experiments. Maintenance of mitochondrial integrity is particularly critical for brain microvascular endothelial cells, which require substantial ATP to sustain blood-brain barrier functions, including tight junction stability and ion homeostasis [16]. Therefore, NBP's mitochondrial protective effect may contribute to the preservation of blood-brain barrier integrity and cerebral microcirculation following ischemic injury.

Regarding the HIF1α/VEGF pathway, OGD alone did not significantly increase HIF1α protein levels in our experimental setting. This observation is consistent with previously described negative feedback mechanisms during prolonged hypoxia, including PHD overactivation and *HIF1α* mRNA destabilization by tristetraprolin in endothelial cells [17,18]. In contrast, NBP treatment following OGD significantly increased HIF1α protein expression ($p < 0.01$), accompanied by upregulation of VEGFR2 protein ($p < 0.05$) and increased *VEGFA* and *eNOS* mRNA levels ($p < 0.05$) (Fig. 4), indicating that NBP actively enhances the HIF1α/VEGF signaling axis rather than merely supporting endogenous hypoxic responses. Although these molecular changes suggest a pro-angiogenic effect, direct functional validation through tube formation or sprouting assays was not performed in this study and will be an important focus of future work. Notably, unlike exogenous VEGF administration, which has been associated with vascular permeability and hemorrhagic complications in clinical trials [19,20], NBP's approach of promoting endogenous VEGF signaling through HIF1α upregulation may better preserve physiological regulatory mechanisms, though this hypothesis requires further *in vivo* verification.

The relationship between HIF1α and inflammation is particularly relevant in stroke. The crosstalk between HIF1α and COX2 pathways may involve shared transcriptional regulators (Fig. 6). Both HIF1α and COX2 are NFκB target genes [21,22,23,24], yet NBP exhibited differential

effects—upregulating HIF1α protein expression while suppressing COX2. The mechanism underlying this selectivity was not directly investigated in the present study. Possible explanations include differential post-translational regulation (e.g., modulation of PHD-mediated hydroxylation affecting HIF1α protein levels) or selective effects on NFκB transcriptional activity toward different target genes; however, these hypotheses require future experimental verification using hydroxylation-specific antibodies, PHD/VHL activity assays, and NFκB nuclear translocation analysis. Notably, chronic inflammation can impair HIF1α signaling through PHD activation, while HIF1α activation promotes anti-inflammatory M2 polarization [25,26]. NBP's simultaneous modulation of pro-angiogenic and anti-inflammatory pathways therefore represents a significant advantage over single-target approaches, creating a favorable microenvironment where pro-angiogenic signaling is enhanced while excessive inflammation is suppressed.

These pathways are intimately connected: chronic inflammation impairs HIF1α signaling through PHD enzyme activation [27,28], while inflammation-induced oxidative stress damages VEGF protein [29]. Conversely, HIF1α activation promotes macrophage polarization toward anti-inflammatory M2 phenotype [25,26], and improved angiogenesis reduces hypoxia-induced inflammatory signals [25,30]. NBP's preservation of mitochondrial function provides an additional mechanistic link, as mitochondrial dysfunction releases DAMPs that activate inflammatory cascades while impairing cellular energy status necessary for VEGF-driven angiogenesis [15,31,32].

This multi-target approach distinguishes NBP from selective COX2 inhibitors, which showed neuroprotection in experimental models but caused cardiovascular side effects in clinical trials [33,34], and from exogenous VEGF administration, which failed in clinical trials due to vascular permeability concerns [19,20]. A randomized, double-blind trial (573 patients) evaluated 90-day sequential administration of intravenous followed by oral NBP for acute ischemic stroke, and found that the NBP sequential therapy group showed improved functional outcomes compared to controls [35].

Several limitations of this study should be acknowledged. First, our findings are derived from a single endothelial cell line (HBMECs) subjected to OGD/R conditions, which does not fully recapitulate the complexity of the neurovascular unit, particularly the interactions between endothelial cells, neurons, astrocytes, pericytes, and immune cells [36,37]. Co-culture models incorporating these cell types would better simulate the *in vivo* blood-brain barrier microenvironment. Second, our study relied exclusively on molecular and biochemical endpoints (Western blot, qPCR, flow cytometry, ELISA, and MitoTracker fluorescence) without direct functional validation. Future studies should incorporate tube formation, migration, and barrier integrity assays (e.g., TEER measurement and permeability to fluorescent tracers), as well as functional inflammatory readouts such as endothelial permeability and leukocyte adhesion, to confirm the biological significance of the observed molecular changes. Third, the mechanism by which NBP upregulates HIF-1α protein levels was not elucidated; whether this occurs through transcriptional activation, translational enhancement, or inhibition of proteasomal degradation (e.g., via PHD or VHL modulation) remains to be determined. Fourth, although *NFκB* mRNA levels were measured, NFκB activation, nuclear translocation, and transcriptional activity were not directly assessed; therefore, the proposed role of NFκB as a shared regulatory node remains a literature-derived hypothesis. Fifth, our study focused on acute effects; long-term impacts on sustained angiogenesis, vascular remodeling, and chronic inflammation require investigation. Finally, in vivo validation using animal models of cerebral ischemia is essential to establish the translational relevance of these findings.

Future research should prioritize *in vivo* validation using stroke models (tMCAO, photothrombotic) to assess NBP's effects on infarct size, blood-brain barrier integrity, and neurological deficits [38]. Advanced imaging (magnetic resonance imaging [MRI] with gadolinium, MR angiography) and two-photon microscopy could provide non-invasive assessment of cerebrovascular effects [39]. Combination studies with tPA or mechanical thrombectomy could evaluate synergistic benefits and safety profiles [40,41]. Multi-omics approaches (scRNA-seq, proteomics, metabolomics) could comprehensively map NBP's effects and identify novel mechanisms [42,43]. Clinical biomarker studies measuring circulating HIF1α, VEGF, and inflammatory markers could identify patients most likely to benefit and provide early treatment response indicators [44,45]. Finally, structure-activity relationship studies could guide development of next-generation derivatives with enhanced properties [46,47].

5. Conclusion

This study provides preliminary *in vitro* evidence that NBP protects brain microvascular endothelial cells against OGD injury through coordinated modulation of cell survival, mitochondrial function, angiogenesis-related signaling, and inflammatory responses. Mechanistically, NBP upregulated HIF1α protein expression and downstream VEGF pathway components while simultaneously suppressing COX2-mediated inflammation, demonstrating a dual pathway modulation strategy that distinguishes it from single-target approaches. These findings may partially explain the multi-faceted protective effects of NBP observed in preclinical studies; however, the precise mechanisms underlying HIF1α upregulation and the selectivity between pro-angiogenic and anti-inflammatory modulation remain to be elucidated. Clinical relevance requires further validation through functional assays, *in vivo* cerebral ischemia models, and clinical investigations.

Availability of Data and Materials

Raw data in this paper was dropped in:https://doi.org/10.6084/m9.figshare.31329709.

Author Contributions

LZ designed the project. YW built the model, performed the tests, and collected and analyzed the data. CS interpreted the results and drafted the manuscript. SC contributed to technical and methodological support. TC collect the data. ZL contributed to the design of the work. LZ and ZL are mainly responsible for obtaining funding and LZ supervising all aspects of the project. All authors contributed to editorial changes in the manuscript. All authors read and approved the final manuscript. All authors have participated sufficiently in the work and agreed to be accountable for all aspects of the work.

Ethics Approval and Consent to Participate

Not applicable.

Acknowledgment

We extend our appreciation to Professor Marong Fang and Doctor Nashwa Amin from Zhejiang University School of Medicine for their technical assistance, facilities and support throughout this study.

Funding

This study received funding from the Hebei Provincial Natural Science Foundation of China (No. H2019206406).

Conflicts of Interest

The authors declare no conflicts of interest.

Supplementary Material

Supplementary material associated with this article can be found, in the online version, at https://doi.org/10.31083/JIN51032.

References

[1] Feigin VL, Brainin M, Norrving B, Martins S, Sacco RL, Hacke W, et al. World Stroke Organization (WSO): Global Stroke Fact Sheet 2022. International Journal of Stroke : Official Journal of the International Stroke Society. 2022; 17: 18–29. https://doi.org/10.1177/17474930211065917

[2] Xiong Y, Wakhloo AK, Fisher M. Advances in Acute Ischemic Stroke Therapy. Circulation Research. 2022; 130: 1230–1251. https://doi.org/10.1161/CIRCRESAHA.121.319948

[3] Tsivgoulis G, Katsanos AH, Sandset EC, Turc G, Nguyen TN, Bivard A, et al. Thrombolysis for acute ischaemic stroke: current status and future perspectives. The Lancet. Neurology. 2023; 22: 418–429. https://doi.org/10.1016/S1474-4422(22)00519-1

[4] Dong T, Li M, Gao F, Wei P, Wang J. Construction and imaging of a neurovascular unit model. Neural Regeneration Research. 2022; 17: 1685–1694. https://doi.org/10.4103/1673-5374.332131

[5] Tiedt S, Buchan AM, Dichgans M, Lizasoain I, Moro MA, Lo EH. The neurovascular unit and systemic biology in stroke - implications for translation and treatment. Nature Reviews Neurology. 2022; 18: 597–612. https://doi.org/10.1038/s41582-022-00703-z

[6] Wang X, Shen Y, Shang M, Liu X, Munn LL. Endothelial mechanobiology in atherosclerosis. Cardiovascular Research. 2023; 119: 1656–1675. https://doi.org/10.1093/cvr/cvad076

[7] Marti HJ, Bernaudin M, Bellail A, Schoch H, Euler M, Petit E, et al. Hypoxia-induced vascular endothelial growth factor expression precedes neovascularization after cerebral ischemia. The American Journal of Pathology. 2000; 156: 965–976. https://doi.org/10.1016/S0002-9440(10)64964-4

[8] Chen X, Qian W, Zhang Y, Zhao P, Lin X, Yang S, et al. Ginsenoside CK cooperates with bone mesenchymal stem cells to enhance angiogenesis post-stroke via GLUT1 and HIF-1α/VEGF pathway. Phytotherapy Research : PTR. 2024; 38: 4321–4335. https://doi.org/10.1002/ptr.8235

[9] Mollace V, Muscoli C, Masini E, Cuzzocrea S, Salvemini D. Modulation of prostaglandin biosynthesis by nitric oxide and nitric oxide donors. Pharmacological Reviews. 2005; 57: 217–252. https://doi.org/10.1124/pr.57.2.1

[10] Basini G, Grasselli F. Nitric oxide in follicle development and oocyte competence. Reproduction (Cambridge, England). 2015; 150: R1–R9. https://doi.org/10.1530/REP-14-0524

[11] Li S, Zhao J, Xi Y, Ren J, Zhu Y, Lu Y, et al. Dl-3-n-butylphthalide exerts neuroprotective effects by modulating hypoxia-inducible factor 1-alpha ubiquitination to attenuate oxidative stress-induced apoptosis. Neural Regeneration Research. 2023; 18: 2424–2428. https://doi.org/10.4103/1673-5374.371366

[12] Yang W, Li L, Huang R, Pei Z, Liao S, Zeng J. Hypoxia inducible factor-1alpha mediates protection of DL-3-n-butylphthalide in brain microvascular endothelial cells against oxygen glucose deprivation-induced injury. Neural Regeneration Research. 2012; 7: 948–954. https://doi.org/10.3969/j.issn.1673-5374.2012.12.012

[13] Wei ZZ, Chen D, Lee MJH, Zhao Y, Gu X, Yu SP, et al. DL-3-n-butylphthalide Increases Collateriogenesis and Functional Recovery after Focal Ischemic Stroke in Mice. Aging and Disease. 2021; 12: 1835–1849. https://doi.org/10.14336/AD.2020.1226

[14] Attwell D, Buchan AM, Charpak S, Lauritzen M, Macvicar BA, Newman EA. Glial and neuronal control of brain blood flow. Nature. 2010; 468: 232–243. https://doi.org/10.1038/nature09613

[15] West AP, Shadel GS, Ghosh S. Mitochondria in innate immune responses. Nature Reviews. Immunology. 2011; 11: 389–402. https://doi.org/10.1038/nri2975

[16] Zlokovic BV. The blood-brain barrier in health and chronic neurodegenerative disorders. Neuron. 2008; 57: 178–201. https://doi.org/10.1016/j.neuron.2008.01.003

[17] Ginouvès A, Ilc K, Macías N, Pouysségur J, Berra E. PHDs overactivation during chronic hypoxia "desensitizes" HIFalpha and protects cells from necrosis. Proceedings of the National Academy of Sciences of the United States of America. 2008; 105: 4745–4750. https://doi.org/10.1073/pnas.0705680105

[18] Chamboredon S, Ciais D, Desroches-Castan A, Savi P, Bono F, Feige JJ, et al. Hypoxia-inducible factor-1α mRNA: a new target for destabilization by tristetraprolin in endothelial cells. Molecular Biology of the Cell. 2011; 22: 3366–3378. https://doi.org/10.1091/mbc.E10-07-0617

[19] Ergul A, Alhusban A, Fagan SC. Angiogenesis: a harmonized target for recovery after stroke. Stroke. 2012; 43: 2270–2274. https://doi.org/10.1161/STROKEAHA.111.642710

[20] Greenberg DA, Jin K. VEGF and ALS: the luckiest growth factor? Trends in Molecular Medicine. 2004; 10: 1–3. https://doi.org/10.1016/j.molmed.2003.11.006

[21] Iadecola C, Anrather J. The immunology of stroke: from mech-

anisms to translation. Nature Medicine. 2011; 17: 796–808. https://doi.org/10.1038/nm.2399
[22] Lambertsen KL, Biber K, Finsen B. Inflammatory cytokines in experimental and human stroke. Journal of Cerebral Blood Flow and Metabolism : Official Journal of the International Society of Cerebral Blood Flow and Metabolism. 2012; 32: 1677–1698. https://doi.org/10.1038/jcbfm.2012.88
[23] Lawrence T. The nuclear factor NF-kappaB pathway in inflammation. Cold Spring Harbor Perspectives in Biology. 2009; 1: a001651. https://doi.org/10.1101/cshperspect.a001651
[24] Liu T, Zhang L, Joo D, Sun SC. NF-κB signaling in inflammation. Signal Transduction and Targeted Therapy. 2017; 2: 17023. https://doi.org/10.1038/sigtrans.2017.23
[25] Krock BL, Skuli N, Simon MC. Hypoxia-induced angiogenesis: good and evil. Genes & Cancer. 2011; 2: 1117–1133. https://doi.org/10.1177/1947601911423654
[26] Cheng SC, Quintin J, Cramer RA, Shepardson KM, Saeed S, Kumar V, et al. mTOR- and HIF-1α-mediated aerobic glycolysis as metabolic basis for trained immunity. Science (New York, N.Y.). 2014; 345: 1250684. https://doi.org/10.1126/science.1250684
[27] Takeda N, O'Dea EL, Doedens A, Kim JW, Weidemann A, Stockmann C, et al. Differential activation and antagonistic function of HIF-{alpha} isoforms in macrophages are essential for NO homeostasis. Genes & Development. 2010; 24: 491–501. https://doi.org/10.1101/gad.1881410
[28] Talks KL, Turley H, Gatter KC, Maxwell PH, Pugh CW, Ratcliffe PJ, et al. The expression and distribution of the hypoxia-inducible factors HIF-1alpha and HIF-2alpha in normal human tissues, cancers, and tumor-associated macrophages. The American Journal of Pathology. 2000; 157: 411–421. https://doi.org/10.1016/s0002-9440(10)64554-3
[29] Otrock ZK, Mahfouz RAR, Makarem JA, Shamseddine AI. Understanding the biology of angiogenesis: review of the most important molecular mechanisms. Blood Cells, Molecules & Diseases. 2007; 39: 212–220. https://doi.org/10.1016/j.bcmd.2007.04.001
[30] Xiong Y, Mahmood A, Chopp M. Angiogenesis, neurogenesis and brain recovery of function following injury. Current Opinion in Investigational Drugs (London, England : 2000). 2010; 11: 298–308.
[31] Zhang Q, Raoof M, Chen Y, Sumi Y, Sursal T, Junger W, et al. Circulating mitochondrial DAMPs cause inflammatory responses to injury. Nature. 2010; 464: 104–107. https://doi.org/10.1038/nature08780
[32] Zhou R, Yazdi AS, Menu P, Tschopp J. A role for mitochondria in NLRP3 inflammasome activation. Nature. 2011; 469: 221–225. https://doi.org/10.1038/nature09663
[33] Candelario-Jalil E, González-Falcón A, García-Cabrera M, Alvarez D, Al-Dalain S, Martínez G, et al. Assessment of the relative contribution of COX-1 and COX-2 isoforms to ischemia-induced oxidative damage and neurodegeneration following transient global cerebral ischemia. Journal of Neurochemistry. 2003; 86: 545–555. https://doi.org/10.1046/j.1471-4159.2003.01812.x
[34] Bresalier RS, Sandler RS, Quan H, Bolognese JA, Oxenius B, Horgan K, et al. Cardiovascular events associated with rofecoxib in a colorectal adenoma chemoprevention trial. The New England Journal of Medicine. 2005; 352: 1092–1102. https://doi.org/10.1056/NEJMoa050493
[35] Cui LY, Zhu YC, Gao S, Wang JM, Peng B, Ni J, et al. Ninety-day administration of dl-3-n-butylphthalide for acute ischemic stroke: a randomized, double-blind trial. Chinese Medical Journal. 2013; 126: 3405–3410.
[36] Iadecola C. The Neurovascular Unit Coming of Age: A Journey through Neurovascular Coupling in Health and Disease. Neuron. 2017; 96: 17–42. https://doi.org/10.1016/j.neuron.2017.07.030
[37] Sweeney MD, Zhao Z, Montagne A, Nelson AR, Zlokovic BV. Blood-Brain Barrier: From Physiology to Disease and Back. Physiological Reviews. 2018; 99: 21–78. https://doi.org/10.1152/physrev.00050.2017
[38] Fluri F, Schuhmann MK, Kleinschnitz C. Animal models of ischemic stroke and their application in clinical research. Drug Design, Development and Therapy. 2015; 9: 3445–3454. https://doi.org/10.2147/DDDT.S56071
[39] Schaffer CB, Friedman B, Nishimura N, Schroeder LF, Tsai PS, Ebner FF, et al. Two-photon imaging of cortical surface microvessels reveals a robust redistribution in blood flow after vascular occlusion. PLoS Biology. 2006; 4: e22. https://doi.org/10.1371/journal.pbio.0040022
[40] Emberson J, Lees KR, Lyden P, Blackwell L, Albers G, Bluhmki E, et al. Effect of treatment delay, age, and stroke severity on the effects of intravenous thrombolysis with alteplase for acute ischaemic stroke: a meta-analysis of individual patient data from randomised trials. Lancet (London, England). 2014; 384: 1929–1935. https://doi.org/10.1016/S0140-6736(14)60584-5
[41] Goyal M, Menon BK, van Zwam WH, Dippel DWJ, Mitchell PJ, Demchuk AM, et al. Endovascular thrombectomy after large-vessel ischaemic stroke: a meta-analysis of individual patient data from five randomised trials. Lancet (London, England). 2016; 387: 1723–1731. https://doi.org/10.1016/S0140-6736(16)00163-X
[42] Vanlandewijck M, He L, Mäe MA, Andrae J, Ando K, Del Gaudio F, et al. A molecular atlas of cell types and zonation in the brain vasculature. Nature. 2018; 554: 475–480. https://doi.org/10.1038/nature25739
[43] Aebersold R, Mann M. Mass-spectrometric exploration of proteome structure and function. Nature. 2016; 537: 347–355. https://doi.org/10.1038/nature19949
[44] Worthmann H, Tryc AB, Deb M, Goldbecker A, Ma YT, Tountopoulou A, et al. Linking infection and inflammation in acute ischemic stroke. Annals of the New York Academy of Sciences. 2010; 1207: 116–122. https://doi.org/10.1111/j.1749-6632.2010.05738.x
[45] Perini F, Morra M, Alecci M, Galloni E, Marchi M, Toso V. Temporal profile of serum anti-inflammatory and pro-inflammatory interleukins in acute ischemic stroke patients. Neurological Sciences : Official Journal of the Italian Neurological Society and of the Italian Society of Clinical Neurophysiology. 2001; 22: 289–296. https://doi.org/10.1007/s10072-001-8170-y
[46] Di L, Kerns EH. Drug-like properties: concepts, structure design, and methods. Elevier: London, UK. 2016.
[47] Schneider G, Fechner U. Computer-based de novo design of drug-like molecules. Nature Reviews. Drug Discovery. 2005; 4: 649–663. https://doi.org/10.1038/nrd1799